

LASERS IN CHEMISTRY

Optical probes and reaction starters

Volume 1: Lasers as probes in chemistry



9

Tunable Diode Laser Absorption Spectroscopy

Peter Werle, Francesco D'Amato and Silvia Viciani

9.1

Semiconductor Lasers

A prerequisite for spectrometers and the applications described in this chapter is diode lasers. In the past, semiconductor lasers, regardless of their operating wavelength, relied upon direct band-to-band transitions in bulk material, where electrons recombine at a p–n junction with positively charged ‘holes’ to release single photons with a wavelength that is determined by the bandgap between the conduction and the valence bands, typical of the chemical composition of the semiconductor sandwich. A tunable diode laser (TDL) consists basically of a crystal on which a p–n junction (homojunction) is formed. The front and rear facets of the cleaved crystal ($\sim 0.01 \text{ mm}^2$) form a laser cavity and do not need reflective coatings, as the Fresnel reflection is sufficiently strong. If electrodes are connected to the top and bottom surfaces and a suitable current (5 mA up to 5 A) is injected through the junction, lasing action takes place. The emission wavelength of diode lasers ranges from the near infrared (NIR) for GaAs to mid-infrared (MIR) for lead-salt diode lasers (Chapter 1), and for each material system it depends on the crystal temperature. Homojunction laser devices have many disadvantages such as poor mode structure and operation around liquid nitrogen temperatures in the MIR. In order to obtain higher operating temperatures, single-mode operation and better beam quality, several improvements have been achieved. Double and buried heterostructure devices have been realized by molecular beam epitaxy (MBE), which allows laser structures to grow in an ordered manner. Therefore, these structures show a much better optical and carrier confinement in the active region, compared to diffused homojunction lasers [3]. Lasers of this type are available between 3050 and 900 cm^{-1} ($3.3\text{--}11.1 \mu\text{m}$), with typical power of a few hundred microwatts. At a particular drive current, the output consists of a series of longitudinal modes separated in wavenumber by $1/2 nL$, where n is the refractive index of the active layer (~ 5) and L is the cavity length ($\sim 0.03 \text{ cm}$). In order to obtain higher spectral purity, lasers are either provided with an internal dispersive element (distributed feedback (DFB) and distributed Bragg reflector (DBR)), or an

external grating is coupled to the laser cavity, in a Littman or Littrow configuration. DFB and DBR cavity designs use, respectively, a corrugated structure, distributed along the entire cavity, and a sequence of dielectric layers with different refractive indices at each end (the latter solution is used for the realization of the so-called vertical-cavity surface-emitting laser (VCSEL) [4], see also Chapter 1). Owing to the Bragg condition, these structures act as distributed or discrete reflectors, but only at specific wavelengths.

Diode lasers are tuned by changing the temperature of the active region, by varying either the temperature of the heat sink on which the diode is mounted, or the laser drive current, which varies the ohmic heating of the active region. Temperature changes allow a slow tuning of the laser over its entire range. Changes in the drive current give a restricted tuning range, of the order of 2 cm^{-1} , but allow modulation of the laser frequency. In practice, the two methods are used in combination, as the laser modes tune through the dependence of the refractive index, n , on both the temperature and the carrier density, which vary with the laser drive current. At low modulation frequencies, the temperature variation of n dominates. At high frequencies ($>1 \text{ MHz}$), thermal inertia reduces the amplitude of the temperature modulation, and carrier-density modulation takes over. A typical value for the current tuning rate is 1 GHz mA^{-1} ($0.03 \text{ cm}^{-1} \text{ mA}^{-1}$), while temperature tuning rate is up to 30 GHz K^{-1} ($1 \text{ cm}^{-1} \text{ K}^{-1}$). With these tuning rates, measurements at a reduced pressure linewidth of 0.005 cm^{-1} (see Table 9.1) require a stability level for temperature of about 1 mK . Therefore, a precise temperature control is always needed.

Quantum cascade lasers (QCLs) are based on a completely different approach than the lasers described so far (Chapter 3). Their operation is based on intersubband transitions, that is, transitions within the conduction band of a cascaded multiple quantum well structure. Although the basic concept was proposed as early as 1971, it took more than 20 years until an actual device was demonstrated in 1994 [5]. In a pictorial way, this laser is freed from the bandgap slavery, as the emission wavelength depends only on the layer thickness and not on the bandgap of the constituent materials. The different materials of the semiconductor in the active region have different band gaps, which leads to the creation of quantum wells. These quantum wells have discrete energy levels due to the thinness of the layers comparable to the electron de Broglie wavelength. The electron motion is restricted in a direction perpendicular to the plane of the layers. The energy levels are determined by the thickness of the layers in the active region. The stages of the QCL consist of an area with closely spaced layers (the injection region) followed by more widely spaced layers (active region). In a QCL, typically 30–75 alternating structures of active and injector/relaxation regions are stacked. Once an electron is injected, it is forced to pass through all the periods of the active regions and injectors sequentially (cascading). Once the device exceeds lasing threshold, it will emit one photon per period. In this way, QCLs can provide more than a thousand times the output power of any other semiconductor laser operating in the MIR and can operate in a large number of modes at wavelengths around the one determined by the energy difference between the upper and intermediate levels. Again, to

Table 9.1 Calculated detection limits for atmospheric constituents for a sampling pressure of 30 mbar and $T = 296$ K based on a minimum detectable absorbance of 10^{-5} and a 100 m path length

Species	λ (μm)	ν (cm^{-1})	S (10^{-19} cm/molecule)	γ_ν (10^{-3} cm^{-1})	γ_ν (MHz)	σ (10^{-17} $\text{cm}^2/\text{molecule}$)	DL (pptv)
O ₃	9.50	1053	0.42	2.64	79.2	0.53	260
N ₂ O	7.69	1301	1.56	2.77	83.1	1.92	70
CO	4.65	2151	1.89	3.85	115.5	1.85	73
CH ₄	7.56	1322	0.53	3.25	97.5	0.60	225
NO	5.33	1876	0.34	3.26	97.8	0.39	350
SO ₂	7.29	1372	0.49	3.86	115.8	0.41	330
NO ₂	6.25	1600	2.18	2.90	87.0	2.70	50
NH ₃	10.74	931	5.20	2.92	87.6	6.18	23
HNO ₃	5.81	1722	0.72	3.75	112.5	0.25	218
HF	1.24	7856	0.76	12.09	362.7	0.27	500
HCl	3.40	2945	5.03	4.30	129.0	4.51	30
HBr	3.78	2649	0.45	2.90	87.0	0.57	240
HI	4.39	2278	0.02	2.21	66.3	0.03	4000
ClO	11.6	860	0.08	2.73	81.9	0.09	1500
OCS	4.87	2053	10.30	3.55	106.5	10.00	13
HCHO	3.56	2781	1.19	5.17	155.1	0.84	160
HCN	3.00	3337	3.69	5.97	179.1	2.33	58
CH ₃ Cl	3.29	3040	0.02	4.12	123.6	0.02	7800
H ₂ O ₂	7.79	1284	0.45	3.52	105.6	0.43	320
C ₂ H ₂	3.07	3260	2.29	5.43	162.9	1.65	83
H ₂ S	7.33	1365	0.01	4.89	146.7	0.007	20000
HCOOH	8.98	1113	0.44	3.32	99.6	0.44	310
HO ₂	7.08	1411	0.12	3.63	108.9	0.11	1200

produce stable, single-mode emission from these QCLs, the DFB configuration is adopted.

First QCLs operated in the continuous wave (CW) mode at cryogenic temperatures [5] and strong efforts have been made towards thermoelectrically cooled devices. Operation at room temperature (RT) has been achieved first in pulsed mode and used for practical applications [6, 7]. For high-resolution spectroscopy, lasers should operate preferably in the CW mode, in which case linewidths of a few kilohertz [8] and even a few hertz [9] can be attained. RT CW emission of up to 17 mW at 9.1 μm was reported for the first time in 2002 [10]. In any case, the choice between pulsed and CW sources is still an open question [11]. Other developments are in progress mainly towards broader gain and emission curves. They are obtained by including, in the same laser, several active regions with slightly different spacings of the layers. The selection of a particular wavelength in such a wide range can be obtained either by multiple DFB gratings [12] or by applying an external cavity [13].

Semiconductor laser devices emitting in the NIR and visible spectral region are also increasingly used [14]. Currently, these lasers are available from blue, based on GaN [15], to 2.3 μm , based on InGaAlAs/InP [16], and even upto 2.8 μm , based on lateral metal Bragg grating in GaAs, InP and GaSb [17]. The latter devices have been qualified for space applications, and will be employed by National Aeronautics and Space Administration (NASA) in the mission to Mars in 2009 for detection of H_2O and CO_2 [18]. The specific features of VCSELs (low consumption, high spectral purity, low dimensions) are opening further fields of applications [19]. Infrared radiation can also be obtained by beating a TDL with another TDL, or a different kind of laser (e.g. Nd:YAG), in a nonlinear crystal such as lithium niobate, for difference frequency generation (DFG) (see [20] and Chapter 7).

9.2

Principles of Diode Laser Spectroscopy

9.2.1

Line Parameters and Selection of Absorption Lines

Beer–Lambert law links the decrease in light power when passing through a sample, to the physical characteristics and the concentration of the absorber(s), and to the interaction length between light and the sample:

$$I_{\text{out}}(\nu) = I_{\text{in}}(\nu) \cdot e^{-Sg(\nu)NL} \quad (9.1)$$

where $I_{\text{out/in}}$ is the power at the exit/entrance of the sample, S is the line strength, $g(\nu)$ is the frequency profile of the absorption, N is the density of the absorbers and L is the interaction length. Pressure affects first of all the number of absorbers, which rises linearly with increasing pressure. The shape of the absorption frequency profile, with increasing pressure, changes from a Doppler profile at low pressures to a Lorentz profile at high pressures, through a Voigt profile at intermediate pressures [21]. A minor effect of the pressure is a shift of the absorption frequencies. As the Voigt profile is a convolution, its use in fitting procedures would require very powerful computing resources. For this reason, several approximations are used, instead [22–24]. The Voigt profile does not take into account the reduction of Doppler width due to collisional narrowing, so sometimes further approximations are used, such as the Galatry profile or the Speed-dependent billiard-ball profile [25]. The effects of temperature are manifold. The density of the sample is inversely proportional to temperature, and the shape of the absorptions depends on temperature both because of the Doppler width and because the pressure broadening depends on temperature [26, 27]. The strengths of the lines depend on temperature because the populations of the levels from which the transitions take place follow the Boltzmann distribution.

The optimum sampling pressure is a compromise between sensitivity and selectivity. As the sampling pressure is reduced, sensitivity does not fall significantly

below the atmospheric pressure value until the point at which Lorentzian and Doppler linewidth are equal, at typical pressures of 10–50 mbar. This is the pressure at which systems are mostly operated. Of course, a strong line is needed to give high sensitivity. The line should be isolated from other lines of the same species, but this is not an absolute requirement and can prove difficult to achieve for the more complex molecules (e.g. nitric acid). The line should also be isolated from interfering lines due either to other trace species (not normally a problem) or to the more abundant atmospheric constituents such as H₂O or CO₂. The task of choosing the operating wavelength is made easier by the availability of spectral line databases [28, 29], of which the most popular is the HITRAN compilation [30].

Q2

9.2.2

Direct Absorption and Modulation Spectroscopy

A straightforward approach to absorption measurements is to sweep the laser repeatedly across an absorption line to analyze the transmission signal. Direct absorption measurements have to resolve small changes in a large signal. This poses severe constraints on the dynamic range of the electronics for the data acquisition. An alternative approach is based on modulation spectroscopy, which is based on the ease with which diode lasers can be modulated [31, 32]. When the laser is modulated through the injection current with a frequency ω_m around its center frequency ω_L , its spectrum is formed by a carrier, plus a series of sidebands, spaced by ω_m . According to the relationship between ω_m and the absorption linewidth, we speak of wavelength modulation spectroscopy (WMS, $\omega_m \sim 50$ kHz), high-frequency wavelength modulation spectroscopy (HFWMS, $\omega_m \sim 5$ MHz) [32] or frequency modulation spectroscopy (FMS, $\omega_m \sim 500$ MHz) [33]. Besides HFWMS, another possibility is to apply two closely spaced modulations ν_1 and ν_2 , both of the order of the absorption linewidth. In this case, an absorption signal is produced at the difference frequency $\nu_1 - \nu_2$, which typically is 10 MHz. Then the technique is termed two-tone frequency modulation spectroscopy (TTFMS) [34]. For FMS, the absorption line is probed by only one or two of these sidebands, whereas for WMS the line is probed by tens of thousands of closely spaced sidebands. The n th harmonic component of the detector signal is proportional to the n th derivative of the absorption line shape, so the technique is known as *derivative*. All harmonics are proportional to species concentration and any can be used for monitoring applications. In a WMS system the electronics is simpler than in FMS, and the detectors are larger, which means easy and stable alignment. Most practical systems adopt WMS with second harmonic. HFWMS technique has been recently adopted in commercial devices [35].

In comparison to direct absorption spectroscopy, the benefits of modulation spectroscopy are twofold. First, it produces a difference signal that is directly proportional to the species concentration (zero baseline technique) and, second, it allows the signal to be detected at a frequency at which the laser noise can be significantly reduced. Despite the noise reduction and the relatively simple experimental setup, the modulation techniques require a calibration; so direct

absorption is often used as the detection technique. In modulation spectroscopy, the signal is directly proportional to the laser power incident on the detector. The noise arises from four sources: detector shot noise, detector thermal noise, laser excess-noise and residual amplitude modulation (RAM) offset noise. Detector shot noise corresponds to the photon noise on the laser power incident on the detector (P). The noise power is proportional to \sqrt{P} and has a white noise frequency spectrum. Detector thermal noise is the signal-independent noise of the detector and preamplifier and depends on the type of detector used. This noise also has a white noise spectrum. Laser excess-noise is the laser noise within the measurement bandwidth centered on the detection frequency [36]. This noise is laser dependent and is influenced by mode competition and by optical feedback to the laser due to scattering from components in the optical system. The noise power spectrum shows approximately $1/f$ dependence and this dependence is the reason that FMS, using a high detection frequency, is potentially a more sensitive technique than WMS [37]. For WMS using second-harmonic detection, laser excess-noise always dominates. For these systems, high laser power is not important because the signal-to-noise ratio (SNR) is not detector-noise limited. In the high-frequency domain where frequency modulation (FM) systems operate, laser excess-noise is negligible [38] and the noise will be dominated by detector thermal noise at low laser powers and by shot noise at higher powers. Where shot noise dominates, the system is said to be quantum noise limited. Such quantum-limited performance has been demonstrated by Gehrtz *et al.* [39] and Werle *et al.* [40] in laboratory measurements using a short absorption path. Since the signal is proportional to P and shot noise to \sqrt{P} , and detector thermal noise is constant, it is clear that for FMS high laser power increases the SNR. This has an impact on the design of the optical system since any transmission losses will reduce the laser power incident on the detector. Therefore, it can be advantageous to use a smaller number of passes of the multipass cell in an FMS system than would be optimum for WMS [41].

9.3 System Design Criteria

9.3.1 Optical Design and Fringes

Typical line strengths are such that even for strongly absorbing species a typical atmospheric concentration of 1 ppbv produces an absorption of only 1 part in 10^7 over a 10 cm path length. Most TDL systems are limited in sensitivity, not by laser or detector noise but by optical fringes superimposed on the measured spectrum [36]. The fringes take the form of an approximately sinusoidal variation of the background signal with a period equal to the free spectral range (FSR) of the étalon formed by two partially reflecting surfaces across the beam. So the most important requirement of the whole optics is to minimize optical fringes. The absorbance variation produced by an étalon formed between two surfaces

of reflectance R is $4R$ (for $R \ll 1$) [42]. Therefore, even surfaces with reflectance as low as 10^{-5} can produce significant fringes. In order to achieve sensitivities in the 10^{-5} – 10^{-6} range methods of reducing the effect of the fringes must be found. These techniques can be categorized as follows: mechanical modulation of the étalon spacing, modified modulation schemes, background subtraction and postdetection signal processing. If the étalon path difference is mechanically modulated [42], or one component forming the étalon is vibrated by a piezoelectric transducer [43], then the fringes will shift relative to the absorption spectrum. As the spectrum is averaged, the fringes will average out, provided the shift amplitude corresponds either to an integral or to a large number of fringes. Cassidy *et al.* [44] have shown that in TDL systems using WMS, the fringes can be averaged to zero by applying an additional low-frequency wavelength modulation to the diode laser, with an amplitude equal to an integral number of periods of the étalon fringes.

For a stable system, a background spectrum obtained by supplying dry nitrogen to the instrument inlet would display the same étalon fringes as the sample spectrum. Subtraction of this background spectrum would then remove the fringes. Real systems, however, are not stable, so the success of background subtraction depends on the thermal and mechanical stability of the system and on the rapidity with which sample and background spectra can be alternated [45]. Stark sample modulation is an approach to modulate the absorption alone without affecting all the other parameters of the signal so that fringes would be automatically removed [46]. In general, the periodic nature of the optical fringes allows analog processing of the signal (such as low-pass filtering) as well as digital processing. Taking the Fourier transform of the averaged spectrum, and then removing the frequency component corresponding to the étalon, before transforming back, can be beneficial in some cases [34]. With a proper choice of the frequency sweep of the laser, the coefficient of the first harmonic can yield the information about the absorption intensity, without back transformation. Fringe profiles from a single étalon can be inserted in the fitting procedure for the retrieval of the line parameters [47].

In order to increase the path length, the first solution is to use a multipass cell. Such cells achieve long paths by using mirrors to fold the optical path, giving typically ~ 100 passes for a 50 cm base length cell. Design criteria are a good compromise among total path length, volume, transmission and quality of the exit beam. A versatile multipass cell was designed by White [48], formed by three spherical mirrors. The total path (L) can be expressed as $4nS$, where n is an integer and S is the mirror separation, depending on the tilt of one of the mirrors. A typical cell of this type would have a 0.5 m mirror separation, a volume of 10 l and a usable path length of 50 m. Owing to the overlap of the beams onto the mirrors, a standing wave can arise every four passes. This will produce a fringe system with a period of $1/4S \text{ cm}^{-1}$ (if S is expressed in centimeters). For a typical cell with $S = 50 \text{ cm}$ the fringe spacing is 0.005 cm^{-1} , or 150 MHz, which is comparable to the absorption linewidth and therefore will be difficult to discriminate against. The Herriott cell [49, 50] consists of two concave mirrors separated by nearly their radius of curvature. The optical beam is injected through a hole in one mirror and is reflected back and forth a number of times before

exiting from the same hole. Unlike the White cell, the beam remains collimated throughout its traversals of the cell. In case of spherical mirrors, the beam traces out circular paths on the two mirrors. This does not give optimum use of the mirror area, and therefore a modified arrangement using slightly astigmatic mirrors is normally used. In this case, the beam traces out a Lissajous figure [51]. If a standing wave is formed by part of the exit beam reentering the cell, the fringes produced will have a much shorter period than the absorption linewidth and can be easily suppressed. A further advantage of the Herriott cell over the White cell is that it is easy to align, since the output beam direction is insensitive to changes in the mirror alignment. A significant disadvantage is that the number of passes is determined by the mirror separation and it is difficult to make this adjustable in any given cell design (but not impossible [52]). The fact that for 100 passes gold-coated mirrors would give a transmission of only 20% must also be taken into account. Multilayer coatings can be used to give improved reflectivity at specific wavelengths.

A different approach to increase the absorption path length is cavity ring down spectroscopy (CRDS), see also Chapter 13. Developed by O'Keefe and Deacon [53], it is based on the measurement of the decay time of photons in a high-finesse cavity. If the molecules inside the cavity absorb photons, the decay time is lowered. As the transmission of the mirrors is of the order of 10^{-4} or less, the effective interaction length is of the order of kilometers. Moreover, the sample volume is very small (in principle, the length of the cavity times the cross-section of the laser beam). The drawback is that only few photons enter (and escape) the cavity, so the power on the detector is very low. This technique underwent several modifications, like cavity-enhanced absorption spectroscopy [54] and intracavity laser absorption spectroscopy. Using the backscatter from the entrance mirror as a feedback forces the laser to emit exactly at a longitudinal cavity mode [55].

Q3 The NICE-OHMS technique combines the enhancement of cavity length of CRDS with the noise reduction of FMS [56], when the modulation applied to the laser is set equal to the FSR of the absorption cavity. Once the laser carrier has been locked to a cavity transmission maximum, the sidebands automatically undergo the same transmission, and can be effectively exploited for FMS detection.

Optoacoustic detection is a completely different approach (see Chapter 8). When a sample absorbs, the power transferred to the internal rovibrational modes degrades to kinetic energy within a timescale of 10^{-8} s. When the laser power is modulated (e.g. by mechanical chopping), or the absorbance is modulated (e.g. by tuning the laser on or off the absorption line), the kinetic energy of the absorbing molecules changes with the same frequency, generating a periodic variation of the sample pressure. A microphone translates the acoustic wave into an electrical signal, and a lock-in amplifier yields the final profile of the absorption. In the past, this technique was applied to CO₂ lasers [57]. As more powerful diode lasers are now available, this technique is applied in several laboratories and applications [58–61].

9.3.2

Calibration, Data Processing and System Performance

The application of modulation techniques does not allow a simple, straightforward calculation of the measured concentration from the measured signal. For an *ab initio* calculation of the absorption signal, a precise knowledge of the line parameters (line strength, linewidth, pressure and temperature dependence) is necessary. Although many molecules have been carefully investigated, some data in the HITRAN database [30] are known with a precision of only about 10–20%. Therefore, many field instruments encompass a calibration system that offers the possibility to generate the necessary reference samples in the absorption cell [62].

Calibration of a gas sensor involves two steps. First the 'zero' must be determined and then the 'span' must be set. Many analytical procedures use pure nitrogen or pure synthetic air to establish the zero point. The next step is the span calibration, and to achieve the best accuracy, a well-defined mixture of the target gas in the ambient air is the best calibration gas. Premixed gas mixtures can be prepared in the laboratory or obtained commercially in various concentrations with a certificate based on reference methods. Polar compounds, such as H_2O_2 , HNO_3 , NH_3 and HCHO , stick to surfaces and, consequently, their mixtures are not stable. For these compounds, permeation-based systems are frequently used to calibrate gas analyzers [63]. Permeation devices are small capsules containing a pure chemical compound in equilibrium between its gas phase and its liquid or solid phase. At a constant temperature, the device emits the compound through its permeable portion at a constant rate. A calibration system for tunable-diode laser spectroscopy (TDLS) field applications requires a source of diluent air, a source of calibration gas, a mixing chamber and a delivery manifold from which analyzers and reference sampling trains can sample the test gas [64]. All components should be allowed sufficient time to stabilize before reference samples are taken and analyzer response is determined. Calibration systems for TDLS have been described [62, 65].

The measurement sequence consists of calibration followed by a series of alternating background and ambient measurements. A background spectrum is then subtracted from the calibration gas spectrum and ambient air spectrum to provide the corrected spectrum. The corrected ambient spectrum can be subjected to various types of étalon fringe removal processing as described in the previous section. The next stage is to determine the ratio between the corrected ambient spectrum and the corrected calibration spectrum. Both exist as a series of digitized values and the most straightforward method is to perform a linear regression. A simple linear regression can be improved by adding linear and quadratic terms and by allowing a wavelength offset between the ambient and calibration spectra [66].

Modulation spectroscopy typically allows a sensitivity of 10^{-5} for a 1 Hz bandwidth. In scanning mode with background subtraction, a complete measurement can be made typically within 1 min. For a given path length and absorbance sensitivity, the detection limit (DL) – defined here as the concentration giving a signal-to-rms-noise ratio of 1 for a particular species – depends only on the

strength (S) and half-width (γ) of the line being used. Table 9.1 gives the spectral parameters for the absorption lines suitable for a range of species. Also shown is the resulting DL assuming an absorbance sensitivity of 10^{-5} and a 100 m path length. The lines shown are not necessarily the strongest for that species, nor do the wavelengths represent the only regions in which the species can be monitored. It is in the nature of field laser applications that optimum performance based on predicted sensitivities, based on line strengths, is not always achieved.

DLs should improve by averaging over a long timescale, but at optical densities near 10^{-6} the sensitivity is usually limited by fringes. Real systems are stable only for a limited time, and therefore will have an optimum averaging time given by temperature drifts, moving fringes, changes in background spectra, and so on.

The performance of a spectrometer can be described using the Allan variance [67]. The Allan variance as a function of the integration time, τ , is the time average of the sample variance of two adjacent averages $A_s(\tau)$ and $A_{s+1}(\tau)$ of time series data x_i :

$$\sigma_A^2(\tau) = \frac{1}{2m} \cdot \sum_{s=1}^m (A_{s+1}(\tau) - A_s(\tau))^2 \quad (9.2)$$

where

$$A_s(\tau) = \frac{1}{k} \cdot \sum_{l=1}^k x_{(s-1)k+l}, \quad s = 1 \dots m$$

An ‘Allan plot’ shows $\sigma_A^2(\tau)$ versus the integration time τ on a log–log scale. At short integration times, in the white-noise dominated region, the square root of the Allan variance is proportional to the DL and, therefore, can be used to predict the DL of a given system as a function of the integration time. The usually observed minimum in the Allan variance corresponds to the optimum integration time, τ_{opt} . If ambient and background spectra are acquired subsequently and the integration times are chosen to be smaller than or equal to the measurement time, system drifts will not influence significantly the quality of the data. τ_{opt} is a characteristic property for a given instrument and is increasingly being used to characterize the performance of spectroscopic trace gas analyzers [11, 62, 68, 69].

9.4

Field Laser Applications in Atmospheric Research

9.4.1

Trace Gas Flux Measurements

A major limitation to atmospheric research on biosphere–atmosphere exchange is the lack of sensitive, reliable and fast-response chemical species sensors. Therefore, in the past, techniques for sensitive trace gas flux measurements based on TDLS

have been developed and successfully applied to micrometeorological flux measurement techniques based on the Eddy covariance technique [70–77]. The availability of such sensors offers a new approach to validate local closed-chamber measurements and provide information about trace gas emissions on a larger scale, which is the basis for any upscaling effort. Ideally, the meteorological conditions controlling the state of the turbulence should not vary over the course of the measurements, and the surface viewed by the sensors should be horizontally uniform, both in its physical and chemical-biological aspects. The Eddy correlation technique directly determines the flux of an atmospheric constituent through a plane that is parallel to the surface. The method may be considered as defining the instantaneous upward or downward transport of the constituent and then averaging contributions to give the net flux, and it must take into account the frequency range of the turbulence for vertically transporting the constituents in the atmosphere. This technique requires simultaneous fast and accurate measurements of the vertical wind velocity and the concentration of the trace species in question. Because of its capability for fast-response measurements, TDLS has been used for flux measurements using the Eddy correlation method. The first step in the Eddy correlation process is to calculate the perturbation values of the data points. For the measured time series of concentration values, c , we can subtract the mean from each data point to yield the time series of perturbations c' . Multiplying these values with the time series of the vertical wind velocity perturbations w' yields a time series $w'c'$. The average of this time series $\langle w'c' \rangle$, gives the turbulent vertical flux, F . An advantage of this method is that it is direct and simple, and fluxes can be calculated at whatever height or location the original time series was measured.

Q4 The time resolution needed for c' and w' in order to achieve an accurate value for F depends on atmospheric conditions, and lengthens with height, but ideally a bandwidth of about 10 Hz is required. Such a response time is easily achieved by a sonic anemometer, which uses ultrasonic sound waves to measure wind speed and direction. The main difficulty is in achieving this fast response from the TDLS concentration measurements. Sachse and coworkers have developed the DACOM instrument [78] which achieved a 70 ms time constant by pumping a 0.581 White cell with a 12001/min engine-driven venturi pump. They have used this on an Electra aircraft to measure CO fluxes over the Amazon basin and also for measuring simultaneous CH₄/CO fluxes over the Alaskan tundra [79]. Verma *et al.* [71] have measured CH₄ fluxes over peatland using a land-based tunable diode laser absorption spectroscopy (TDLAS) with a 100 ms time constant. In what is probably the first reported use of the TTFMS modulation technique for field measurements, Wienhold *et al.* have measured N₂O fluxes from fertilized grassland [80]. The concentration measurements had a 200 ms time constant limited by the cell exchange time. The fast FM spectrometer shown in (Figure 9.1) was used to determine CH₄ emissions in rice paddy fields in Italy and to explore systematic differences between the state-of-the-art closed-chamber method and a direct micrometeorological technique based on Eddy correlation measurements [77]. Recently, this technique has been extended to isotope studies in ecosystem research [81–83].

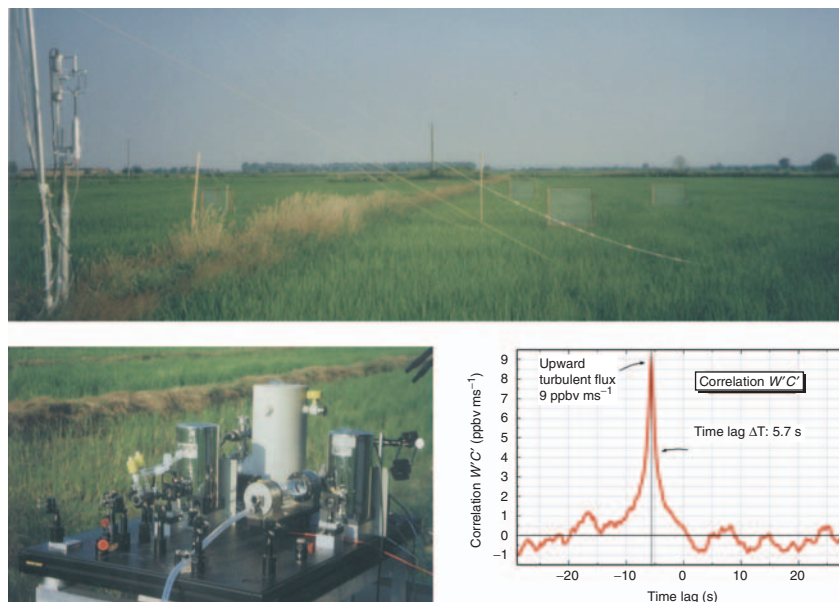


Fig. 9.1 Field measurements of methane emissions from rice paddy fields in Italy. A sonic anemometer and a fast diode-laser spectrometer provide input data for the calculation of the turbulent CH_4 flux [77]. The time lag between the measurement of the vertical wind and the concentration is due to the sampling line delay.

9.4.2

Airborne Atmospheric Measurements

An increasing number of instruments based on diode lasers have been employed for trace gas measurements in the stratosphere and in the troposphere, using both aircraft and balloons as platforms. The fast response time of TDL spectrometers (of the order of 1 s) is essential to observe the fine atmospheric structure of a few kilometers, when the measurements are performed from an aircraft having a cruising speed of hundreds of meters per second. The straightforward design of TDL spectrometers makes possible the fulfilment of the requirements of compactness, weight, portability and totally unattended operation under harsh ambient conditions (vibrations, wide ranges of pressure and temperature, electromagnetic interference), necessary for airborne *in situ* measurements. Stratospheric measurements were already performed in 1983 [84, 85] with the open-path balloon-borne BLISS instrument, based on cryogenic diode lasers and a White cell. Many other TDL spectrometers have been developed for airborne atmospheric research and have been employed during several field campaigns. Most of them are based on cryogenically cooled lead-salt diode lasers in combination with White or Herriott cells. Examples of such type of TDL spectrometers are ATLAS, a device for the measurement of CO or N_2O on board the NASA's ER-2 aircraft [86]; ALIAS,

Q5

an instrument with four channels for the simultaneous measurements of four species among HCl, N₂O, CH₄, NO₂ and HNO₃, always on board the ER-2 [87]; TRISTAR, an analyzer with three channels for simultaneous measurement of CO, N₂O and CH₄ on board the two aircrafts Falcon 20 (German Aerospace Centre, DLR) and Cessna Citation II (operated by the Technical University Delft of The Netherlands) [88]; ARGUS, with two channels for simultaneous measurements of N₂O and CH₄, which owing to its small size has been integrated on many platforms (e.g. NASA ER-2 and WB-57, and also balloons) [89]; and TDLAS, a spectrometer for measurement of HCHO on board NASA's DC-8 aircraft [90].

In the last decade QCLs and DFG sources have been used in airborne atmospheric research, too. The first QCL measurement in the stratosphere was performed in 1999 by the ALIAS instrument, replacing one of the four lead-salt diode lasers with a single-mode QCL-DFB, cooled by liquid nitrogen, emitting at around 7.9 μm. The spectrometer measured CH₄ and N₂O concentrations on board the ER-2 aircraft [91]. Recent laboratory and field studies demonstrated that replacing lead-salt lasers by CW QCLs results in sensitivity improvements of MIR TDLS systems by a factor of 2–3 [92]. Therefore, the TRISTAR spectrometer was equipped with three QCLs, cryogenically cooled, to measure CH₄, CO and HCHO. In October 2005, the modified TRISTAR instrument was installed on a Lear Jet 35A as part of a scientific payload to study the photochemistry over the tropical rainforest in South America during the GABRIEL campaign. A second deployment was during fall 2006 as part of the HOOVER campaign to study HO_x and its precursors in the upper troposphere over Europe. The DL for HCHO was about 500 pptv for a 2 s average, while postflight signal averaging over a 2 min interval resulted in a 150 pptv DL. RT QCLs have already been used for airborne measurements. The QCLs are operated in pulsed mode, which allows thermoelectric cooling [93]. Besides the QCL technology, the development of DFG spectrometers can also be useful to reduce the weight and the size of airborne instruments by removing the cryogenic apparatus. Recently, an airborne spectrometer measuring at 3.5 μm was developed by mixing a DFB diode laser at 1562 nm and a DFB fiber laser at 1083 nm in a periodically poled LiNbO₃ crystal [94]. The instrument was employed for ultrasensitive measurement of HCHO in three consecutive airborne field missions: MIRAGE, IMPEX and TEXAQS2006, utilizing the National Center for Atmospheric Research's C-130 and National Oceanic and Atmospheric Administration's P-3 airborne platforms. The in-flight performance yielded sensitivities between 3 and 20 pptv.

Despite the development of these new lasers sources, spectrometers based on lead-salt diode lasers are still widely employed [95–97]. Also, the recently developed cryogenic operated laser diode (COLD) instrument uses Pb-salt diodes and is designed for airborne measurements of stratospheric trace gas concentrations [47]. It is part of the payload during scientific missions of the M55 Geophysica aircraft, a former Russian high-altitude reconnaissance aircraft capable of operating at an altitude up to 22 km. The COLD instrument uses direct absorption in a multipass Herriott cell with 36 m optical path in conjunction with fast sweep integration. This technique allows absolute concentration measurement without the need for in-flight calibration procedures. Recently, the instrument was successfully

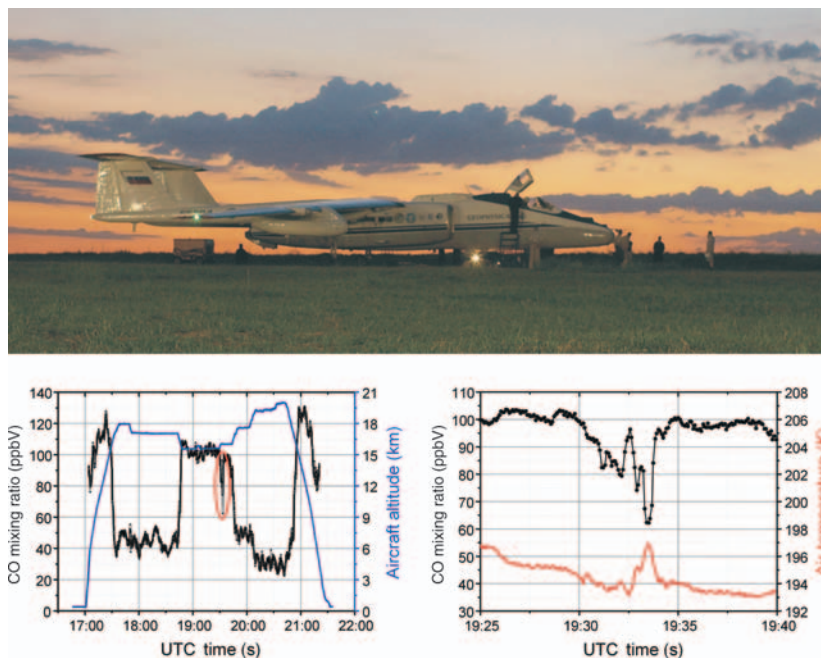


Fig. 9.2 Geophysica M-55 prepared for a measurement flight from Araçatuba (Brazil) with COLD being part of the scientific instrumentation on board. The CO mixing ratio and aircraft altitude are plotted versus universal time (UTC). A zoom of the fine CO structure is shown enlarged to illustrate the high resolution of the spectrometer [47].

employed during three airborne atmospheric research missions: TROCCINOX-2 in Brazil, SCOUT-O3 in Australia and AMMA in Burkina Faso.

The COLD system performance achieved during in-flight operation is a sensitivity of few ppbv with a time resolution of 4 s. A typical COLD result for CO concentration, recorded during a TROCCINOX-2 flight, is shown in (Figure 9.2). For an aircraft speed of about 210 m s^{-1} , the instrument provides CO concentrations with a horizontal resolution of about 850 m, so that atmospheric fine structures can be clearly identified. In general, airborne measurements help to understand the chemistry and transport processes in the troposphere and the stratosphere and provide valuable input for the validation of atmospheric models, with possible important implications for the prediction of the global climate.

9.5

Outlook

The development of high-performance laser sources (long-wavelength DFB, VCSEL, QCL, DFG, etc.) will allow better access to the strong fundamental molecular

Q6 absorption bands. New measurements will be routinely possible or smaller and simpler devices will be commercially available, with respect to the present ones, with the same DLs and resolution. Better DLs are still required for research applications using stable isotope ratio infrared spectroscopy [83, 98, 99]. The advent of terahertz sources is opening the field of detection of drugs and explosives, with important implications for security purposes [p27]. The development of fiber components, mainly amplifiers, can lead to the realization of compact solid-state light detection and ranging (LIDAR) systems, in spectral regions presently not covered by simple sources (Chapter 6). The increase in performance will be hopefully coupled with a reduction in manufacturing costs and may allow the development of sensors networks, for the global measurements of atmospheric trace gases (e.g. Kyoto monitoring of greenhouse gases, concentrations and fluxes) with low installation expenses and low maintenance. For more information on diode laser applications in the process industries the reader is referred to Chapter 10. The same concept applies for medical, noninvasive diagnostics devices, which can become more and more widespread.

9.6

Summary

TDLS has made the transition from a technique mainly of interest to instrument developers to one that produces results of real value to atmospheric research. During the last decade, it has become a technique that can be used even by nonexpert operators. In addition, it is a general technique, as the same instrument can easily be converted from one species to another by changing the laser and the calibration gas. TDLS offers automated measurements at time constants of 1 min or less, and, finally, the time constant can be traded off against sensitivity. A high-resolution spectroscopic technique, it is virtually immune to interferences by other species – a problem that plagues most competing methods. This ability to provide unambiguous measurements leads to the use of TDLS as a reference technique against which other methods are often compared.

References

- Schiff, H.I., Mackay, G.I., Bechara, J. (1994) in (ed M.W. Sigrist), *Air Monitoring by Spectroscopic Techniques*, John Wiley & Sons Ltd, New York; (a) Brassington, D.J. (1994) in (eds R.E. Hester and R.J. Clark), *Spectroscopy in Environmental Science*, Vol. 24, Advances in Spectroscopy, John Wiley & Sons Ltd, New York.
- Werle, P. (2004) Diode-laser sensors for in-situ gas analysis, in *Lasers in Environmental and Life Sciences – Modern Analytical Methods*, (eds P. Hering, P. Lay and S. Stry), Springer Verlag, Heidelberg, pp. 223–43.
- Svelto, O. (1998) *Principles of Lasers*, 4th edn, Springer, Berlin, ISBN: 9780306457487.
- Koyama, F., Kinoshita, S. and Iga, K. (1988) “Room temperature cw operation of GaAs vertical cavity surface emitting laser”. *Transactions on IEICE*, E71, 1089–90.

- 5 Faist, J., Capasso, F., Sivco, D.L., Sirtori, C., Hutchinson, A.L. and Cho, A.Y. (1994) "Quantum cascade laser". *Science*, **264**, 553–56.
- 6 Weidmann, D., Kosterev, A., Roller, C., Curl, R.F., Fraser, M.P. and Tittel, F.K. (2004) "Monitoring of ethylene by a pulsed quantum cascade laser". *Applied Optics*, **43**, 3329–34.
- 7 Manne, J., Sukhorukov, O., Jäger, W. and Tulip, J. (2006) "Pulsed quantum cascade laser-based cavity ring-down spectroscopy for ammonia detection in breath". *Applied Optics*, **45**, 9230–37.
- 8 Williams, R.M., Kelly, J.F., Hartman, J.S., Sharpe, S.W., Taubman, M.S., Hall, J.L., Capasso, F., Gmachl, C., Sivco, D.L., Baillargeon, J.N. and Cho, A.Y. (1999) "Kilohertz linewidth from frequency-stabilized mid-infrared quantum cascade lasers". *Optics Letters*, **24**, 1844–46.
- 9 Taubman, M.S., Myers, T.L., Cannon, B.D., Williams, R.M., Capasso, F., Gmachl, C., Sivco, D.L. and Cho, A.Y. (2002) "Frequency stabilization of quantum-cascade lasers by use of optical cavities". *Optics Letters*, **27**, 2164–66.
- 10 Beck, M., Hofstetter, D., Aellen, T., Faist, J., Oesterle, U., Ilegems, M., Gini, E. and Melchior, H. (2002) "Continuous wave operation of mid-infrared semiconductor laser at room temperature". *Science*, **295**, 301–5.
- 11 McManus, J.B., Nelson, D.D., Herndon, S.C., Shorter, J.H., Zahniser, M.S., Blaser, S., Hvozdar, L., Muller, A., Giovannini, M. and Faist, J. (2006) "Comparison of CW and pulsed operation with a TE-cooled quantum cascade infrared laser for detection of nitric oxide at 1900 cm^{-1} ". *Applied Physics B*, **85**, 235–41.
- 12 Wittmann, A., Giovannini, M., Faist, J., Hvozdar, L., Blaser, S., Hofstetter, D. and Gini, E. (2006) "Room temperature, continuous wave operation of distributed feedback quantum cascade lasers with widely spaced operation frequencies". *Applied Physics Letters*, **89**, 141116.
- 13 Day, T., Arnone, D., Crivello, S.F. and Weida, M.J. (2006) *Miniaturized External Cavity Quantum Cascade Lasers for Broad Tunability in the Mid-infrared*, in CLEO/QELS 06 Technical Digest (CD), paper CTuFF5, Optical Society of America.
- 14 Werle, P., Maurer, K., Kormann, R., Mücke, R., D'Amato, F., Lancia, T. and Popov, A. (2002) "Spectroscopic gas analyzers based on indium-phosphide, antimonide and lead-salt diode-lasers". *Spectrochimica Acta A*, **58**, 2361–72.
- 15 Nakamura, S., Senoh, M., Nagahama, S., Iwasa, N., Yamada, T., Matsushita, T., Kiyoku, H. and Sugimoto, Y. (1996) "InGaN-based multi-quantum-well-structure laser diodes". *Japanese Journal Of Applied Physics* **2**, **35** (1B), L74–L76.
- 16 Ortsiefer, M., Böhm, G., Grau, M., Windhorn, K., Rönneberg, E., Roszkopf, J., Shau, R., Dier, O. and Amann, M.C. (2006) "Electrically pumped room temperature CW VCSELs with $2.3\text{ }\mu\text{m}$ emission wavelength". *Electronics Letters*, **42**, 640–41.
- 17 Seufert, J., Fischer, M., Legge, M., Koeth, J., Werner, R., Kamp, M. and Forchel, A. (2004) "DFB laser-diodes in the wavelength range from 760 nm to $2.5\text{ }\mu\text{m}$ ". *Spectrochimica Acta A*, **60**, 3243–47.
- 18 Tarsitano, C. and Webster, C. (2007) "Multi-laser Herriott cell for planetary tunable laser spectrometers". *Applied Optics*, **46**, 6923–35.
- 19 Gulden, K. (2007) "Vertical emission opens new doors for VCSELs". *Optics and Laser in Europe*, **153**, 29–32.
- 20 Pine, A.S. (1977) IR spectroscopy via difference-frequency generation, in *Laser Spectroscopy III*, Vol. 7 (eds J.L. Hall and J.L. Carlsten), *Springer Series in Optical Sciences*, (ed D.L. MacAdam), Springer-Verlag, Berlin, p. 376, ISBN 3-540-08543-2 and ISBN 3-387-08543-2.

- 21 Corney, A. (2006) *Atomic and Laser Spectroscopy*, Chapter 8, Oxford University Press, New York, ISBN13: 9780199211456.
- 22 Puerta, J. and Martin, P. (1981) "Three and four generalized Lorentzian approximations for the Voigt line shape". *Applied Optics*, **20**, 3923–28.
- 23 Whiting, E.E. (1968) "An empirical approximation to the Voigt profile". *Journal of Quantitative Spectroscopy and Radiative Transfer*, **8**, 1379–84.
- 24 Olivero, J.J. and Longbothum, R.L. (1977) "Empirical fits to the Voigt line width: a brief review". *Journal of Quantitative Spectroscopy and Radiative Transfer*, **17**, 233–36.
- 25 Lisak, D., Hodges, J.T. and Ciurylo, R. (2006) "Comparison of semi-classical line-shape models to rovibrational H₂O spectra measured by frequency-stabilized cavity ring-down spectroscopy". *Physical Review*, **A73**, 012507.
- 26 Baldacchini, G., D'Amato, F., Rosa, M.De., Buffa, G. and Tarrini, O. (1995) "Temperature dependence of self broadening of Ammonia transitions in the V₂ Band". *Journal of Quantitative Spectroscopy and Radiative Transfer*, **53**, 671–80.
- 27 Benedetti, R., Giulietti, K. and Rosa-Clot, M. (1998) "Line shape analysis of O₂ in air as a way to measure temperature using a DFB-diode-laser at 761nm". *Optics Communications*, **154**, 47–53.
- 28 McClatchey, R.A., Benedict, W.S., Clough, S.A., Burch, D.E., Fox, K., Rothman, L.A. and Garing, J.S. (1973) *AFCRL Atmospheric Absorption Line Parameters Compilation*, AFCRL-TR-0096.
- 29 Husson, N., Chedin, A., Scott, N.A., Bailly, D., Graner, G., Lacombe, N., Levy, A., Rossetti, C., Tarrago, G., Camy-Peyret, C., Flaud, J.M., Bauer, A., Colmont, J.M., Monnanteuil, N., Hilico, J.C., Pierre, G., Loete, M., Champion, J.P., Rothman, L.S., Brown, L.R., Orton, G., Varanasi, P., Rinsland, C.P., Smith, M.A.H. and Goldman, A. (1986) "The GEISA spectroscopic line parameters data bank". *Annales Geophysicae*, **4**, A, 2, 185–90.
- 30 Rothman, L.S., Jacquemart, D., Barbe, A., Benner, D.C., Birk, M., Brown, L.R., Carleer, M.R., Chackerian, C., Chance, K., Couderth, L.H., Dana, V., Devi, V.M., Flaud, J.M., Gamache, R.R., Goldman, A., Hartmann, J.M., Jucks, K.W., Maki, A.G., Mandin, J.Y., Massie, S.T., Orphal, J., Perrin, A., Rinsland, C.P., Smith, M.A.H., Tennyson, J., Tolchenov, R.N., Toth, R.A., Auwera, J.Vander., Varanasi, P. and Wagner, G. Jr. (2005) "The HITRAN 2004 molecular spectroscopic database". *Journal of Quantitative Spectroscopy and Radiative Transfer*, **96**, 139–204.
- 31 Cooper, D.E. and Warren, R.E. (1987) "Frequency modulation spectroscopy with lead-salt diode lasers: a comparison of single-tone and two-tone techniques". *Applied Optics*, **26**, 3726–32.
- 32 Bomse, D.S., Stanton, A.C. and Silver, J.A. (1992) "Frequency modulation and wavelength modulation spectroscopies: comparison of experimental methods using a lead-salt diode laser". *Applied Optics*, **31**, 718–31.
- 33 Werle, P. (1998) "Review of recent advances in laser based gas monitors". *Spectrochimica Acta*, **A54**, 197–236.
- 34 D'Amato, F. and Rosa, M.De. (2002) "Tunable diode-lasers and two-tone frequency modulation spectroscopy applied to atmospheric gas analysis". *Optics and Lasers in Engineering*, **37**, 533–51.
- 35 D'Amato, F., Chiarugi, A., Fogale, D. and Finardi, G. (2003) *Realization of a Methane Leak Detector for Roads Inspection*. CLEO/EUROPE, Munich (D), 22-27/06/2003, C14M.
- 36 Werle, P. (1995) "Laser excess noise and interferometric effects in frequency modulated diode laser spectrometers". *Applied Physics B*, **60**, 499–506.

- 37 Werle, P., Slemr, F., Gehrtz, M. and Bräuchle, C. (1989) "Wideband noise characteristics of a lead-salt diode laser". *Applied Optics*, **28**, 1638–42.
- 38 Fischer, H. and Tacke, M. (1991) "High-frequency intensity noise of lead-salt diode lasers". *Journal of the Optical Society of America B*, **8**, 1824–30.
- 39 Gehrtz, M., Bjorklund, G.C. and Whittaker, E.A. (1985) "Quantum limited laser frequency-modulation spectroscopy". *Journal of the Optical Society of America B*, **2**, 1510–26.
- 40 Werle, P., Slemr, F., Gehrtz, M. and Bräuchle, C. (1989) "Quantum limited FM-spectroscopy with a lead-salt diode laser: a comparison of theoretical and experimental data". *Applied Physics B*, **49**, 99–108.
- 41 Werle, P. and Slemr, F. (1991) "Signal-to-noise ratio analysis in laser absorption spectrometers using optical multipass cells". *Applied Optics*, **30**, 430–34.
- 42 Webster, C.R. (1985) "Brewster-plate spoiler: a novel method for reducing the amplitude of interference fringes that limit tunable laser absorption sensitivities". *Journal of the Optical Society of America B*, **2**, 1464–70.
- 43 Silver, J.A. and Stanton, A.C. (1988) "Optical interference fringe reduction in laser absorption experiments". *Applied Optics*, **27**, 1914–16.
- 44 Cassidy, D.T. and Reid, J. (1982) "Harmonic detection with tunable diode lasers-two-tone modulation". *Applied Physics B*, **29**, 279–85.
- 45 Werle, P. (1996) "Tunable diode laser absorption spectroscopy: recent findings and novel approaches". *Infrared Physics and Technology*, **37**, 59–66.
- 46 Dyroff, C., Weibring, P., Fried, A., Richter, D., Walega, J., Zahn, A., Freude, W. and Werle, P. (2007) "Stark-enhanced diode laser spectroscopy of Formaldehyde using a modified Herriott-type multipass cell". *Applied Physics B*, **88**, 117–23.
- 47 Viciani, S., D'Amato, F., Mazzinghi, P., Castagnoli, F., Toci, G. and Werle, P. (2007) "A cryogenic operated diode laser spectrometer for airborne measurement of stratospheric trace gases". *Applied Physics B*.
- 48 White, J.U. (1942) "Long optical paths of large aperture". *Journal of the American Optical Association*, **32**, 285–88.
- 49 Herriott, D., Kogelnik, H. and Kompfner, R. (1964) "Off-axis paths in spherical mirror interferometers". *Applied Optics*, **3**, 523–26.
- 50 Herriott, D.R. and Schulte, H.J. (1965) "Folded optical delay lines". *Applied Optics*, **4**, 883–89.
- 51 McManus, J.B., Kebabian, P.L. and Zahniser, M.S. (1995) "Astigmatic mirror multipass absorption cells for long-path-length spectroscopy". *Applied Optics*, **34**, 3336–36.
- 52 D'Amato, F., Clot, M.R., Clot, P.R., Chiarugi, A. and Carrara, S. (2007) Variable length herriott-type multi-pass cell, European patent request N. 07425172.9/EP07425172, 22/03/2007.
- 53 O'Keefe, A. and Deacon, D.A.G. (1988) "Cavity ring-down optical spectrometer for absorption measurements using pulsed laser sources". *The Review of Scientific Instruments*, **59**, 2544.
- 54 Berden, G., Peeters, R. and Meijer, G. (2000) "Cavity ring-down spectroscopy: experimental schemes and applications". *International Reviews in Physical Chemistry*, **19**, 565–607.
- 55 Morville, J., Kassi, S., Chenevier, M. and Romanini, D. (2005) "Fast, low-noise, mode-by-mode, cavity-enhanced absorption spectroscopy by diode laser self-locking". *Applied Physics B*, **80**, 1027–38.
- 56 Schmidt, F.M., Foltynowicz, A., Ma, W. and Axner, O. (2007) "Fiber-laser-based noise-immune cavity-enhanced optical heterodyne molecular spectrometry for Doppler-broadened detection of C₂H₂ in the parts per trillion range". *Journal of the Optical Society of America B*, **24**, 1392–405.
- 57 Brewer, R.J., Bruce, C.W. and Mater, J.L. (1982) "Optoacoustic

- spectroscopy of C₂H₄ at the 9- and 10- μ m ¹²C¹⁶O₂ laser wavelengths". *Applied Optics*, **21**, 4092–100.
- 58 Veres, A., Bozóki, Z., Mohácsi, Á., Szakáll, M. and Szabo, G. (2003) "External cavity diode laser based photoacoustic detection of CO₂ at 1.43 μ m: The effect of molecular relaxation". *Applied Spectroscopy*, **57**, 900–5.
- 59 Kosterev, A.A. and Tittel, F.K. (2004) "Ammonia detection by use of quartz-enhanced photoacoustic spectroscopy with a near-IR telecommunication diode laser". *Applied Optics*, **43**, 6213–17.
- 60 Cattaneo, H., Laurila, T. and Hernberg, R. (2006) "Photoacoustic detection of oxygen using cantilever enhanced technique". *Applied Physics B*, **85**, 337–41.
- 61 Li, J., Gao, X., Fang, L., Zhang, W. and Cha, H. (2007) "Resonant photoacoustic detection of trace gas with DFB diode laser". *Optics and Laser Technology*, **39**, 1144–49.
- 62 Werle, P., Mazzinghi, P., D'Amato, F., Rosa, M.De., Maurer, K. and Slemr, F. (2004) "Signal processing and calibration procedures for in-situ diode laser absorption spectroscopy". *Spectrochimica Acta A*, **60**, 1685–705.
- 63 Nelson, G.O. (1992) *Gas Mixtures: Preparation and Control*, Lewis Publishers.
- 64 Goldan, P.D., Kuster, W.C. and Albritton, D.L. (1986) "A dynamic dilution system for the production of sub-ppb concentrations of reactive and labile species". *Atmospheric Environment*, **20**, 1203–9.
- 65 Fried, A., Lee, Y.N., Frost, G., Wert, B., Henry, B., Drummond, D.R., Hübler, G. and Jobson, T. (2002) "Airborne CH₂O measurements over the North Atlantic during the 1997 NARE campaign: instrument comparisons and distributions". *Journal of Geophysical Research*, **107** D13, 10.
- 66 Werle, P., Scheumann, B. and Schandl, J. (1994) "Real time signal processing concepts for trace gas analysis by TDLAS". *Optical Engineering*, **33**, 3093–105.
- 67 Werle, P., Mücke, R. and Slemr, F. (1993) "The limits of signal averaging in tunable diode laser spectroscopy". *Applied Physics B*, **57**, 131–39.
- 68 Weibring, P., Richter, D., Fried, A., Walega, J.C. and Dyroff, C. (2006) "Ultra-high-precision mid-IR spectrometer II: system description and spectroscopic performance". *Applied Physics B*, **85**, 207–18.
- 69 Lewicki, R., Wysocki, G., Kosterev, A.A. and Tittel, F.K. (2007) "QEPAS based detection of broadband absorbing molecules using a widely tunable, cw quantum cascade laser at 8.4 μ m". *Optics Express*, **15**, 7357–66.
- 70 Fan, S.M., Wofsy, S.C., Bakwin, P.S., Jacob, D.J., Anderson, S.M., Keabian, P.L., McManus, J.B., Kolb, C.E. and Fitzjerald, D.R. (1992) "Micrometeorological measurements of CH₄ and CO₂ exchange between the atmosphere and subarctic tundra". *Journal of Geophysical Research*, **97**, 16627–43.
- 71 Verma, S.B., Ullman, F.G., Billesbach, D., Clement, R.J., Kim, J. and Verry, E.S. (1992) "Eddy correlation measurements of methane flux in a northern peatland ecosystem". *Boundary Layer Meteorology*, **58**, 289–305.
- 72 Edwards, G.C., Neumann, H.H., Hartog, G., Thurtell, G.W. and Kidd, G. (1994) "Eddy correlation measurements of methane fluxes using a tunable diode laser at the Kinosheo Lake tower site during the northern wetlands study (NOWES)". *Journal of Geophysical Research*, **99**, 1511–17.
- 73 Simpson, I.J., Thurtell, G.W., Kidd, G.E., Lin, M., Demertriades-Shah, T.H., Flitcroft, I.D., Kanemasu, E.T., Nie, D., Bronson, K.F. and Neue, H.U. (1995) "Tunable diode laser measurements of methane fluxes from an irrigated rice paddy field in the Philippines". *Journal of Geophysical Research*, **100**, 7283–90.

- 74 Fowler, D., Hargreaves, K.J., Skiba, U., Milne, R., Zahniser, M.S., Moncrieff, J.B., Beverland, I.J. and Gallagher, M.W. (1995) "Measurements of CH₄ and N₂O fluxes at the landscape scale using micrometeorological methods". *Philosophical Transactions of the Royal Society of London*, **351**, 363–70.
- 75 Hovde, D.C., Meyers, T.P., Stanton, A.C. and Matt, D.R. (1995) "Methane emissions from a landfill measured by Eddy correlation using a fast response diode laser sensor". *Journal of Atmospheric Chemistry*, **20**, 141–62.
- 76 Kormann, R., Müller, H. and Werle, P. (2001) "Eddy flux measurements of methane over the fen Murnauer Moos, 11°11'E, 47°39'N, using a fast tunable diode laser spectrometer". *Atmospheric Environment*, **35**, 2533–44.
- 77 Werle, P. and Kormann, R. (2001) "A Fast chemical sensor for Eddy correlation measurements of Methane emissions from rice paddy fields". *Applied Optics*, **40**, 846–58.
- 78 Ritter, J.A., Lenschow, D.H., Barrick, J.D., Gregory, G.L., Sachse, G.W., Hill, G.F. and Woerner, M.A. (1990) "Airborne flux measurements and budget estimates of trace species over the Amazon Basin during the GTE/ABLE-2B Expedition". *Journal of Geophysical Research*, **95D**, 16875–86.
- 79 Ritter, J.A., Barrick, J.D., Watson, C.E., Sachse, G.W., Gregory, G.L., Anderson, B.E., Woerner, M.A. and Collins, J.E. Jr. (1994) "Airborne boundary layer flux measurements of tracespecies over Canadian boreal forest and northern wetland regions". *Journal of Geophysical Research*, **99**, 1671–86.
- 80 Wienhold, F.G., Frahm, H. and Harris, G.W. (1994) "Measurements of N₂O fluxes from fertilised grassland using a fast response tunable diode laser spectrometer". *Journal of Geophysical Research*.
- 81 Bowling, D., Sargent, S., Tanner, B. and Ehleringer, J. (2003) "Tunable diode laser absorption spectroscopy for stable isotope studies of ecosystem–atmosphere CO₂ exchange". *Agricultural and Forest Meteorology*, **118**, 1–19.
- 82 McManus, J.B., Nelson, D.D., Shorter, J.H., Jimenez, R., Herndon, S., Saleska, S. and Zahniser, M. (2005) "A high precision pulsed quantum cascade laser spectrometer for measurements of stable isotopes of carbon dioxide". *Journal Of Modern Optics*, **52**, 2309–21.
- 83 Saleska, S.R., Shorter, J.H., Herndon, S., Jiménez, R., McManus, J.B., Munger, J.W., Nelson, D.D. and Zahniser, M.S. (2006) "What are the instrumentation requirements for measuring the isotopic composition of net ecosystem exchange of CO₂ using Eddy covariance methods?" *Isotopes in Environmental and Health Studies*, **42**, 115–33.
- 84 Menzies, R.T., Webster, C.R. and Hinkley, E.D. (1983) "Balloon-borne diode-laser absorption spectrometer for measurements of stratospheric trace species". *Applied Optics*, **22**, 2655–64.
- 85 Hastie, D.R. and Miller, M.D. (1985) "Balloon-borne tunable diode laser absorption spectrometer for multispecies trace gas measurements in the stratosphere". *Applied Optics*, **24**, 3694–701.
- 86 Podolske, J. and Loewenstein, M. (1993) "Airborne tunable diode laser spectrometer for trace-gas measurement in the lower stratosphere". *Applied Optics*, **32**, 5324–33.
- 87 Webster, C.R., May, R.D., Trimble, C.A., Chave, R.G. and Kendall, J. (1994) "Aircraft (ER-2) laser infrared absorption spectrometer (ALIAS) for in-situ stratospheric measurement of HCl, N₂O, CH₄, NO₂, and HNO₃". *Applied Optics*, **33**, 454–72.
- 88 Wienhold, F.G., Fischer, H., Hoor, P., Wagner, V., Königstedt, R., Harris, G.W., Anders, J., Grisar, R., Knothe, M., Riedel, W.J., Lübken, F.J. and Schilling, T. (1998) "TRISTAR - a tracer in situ TD-LAS for atmospheric research". *Applied Physics B*, **67**, 411–17.

- 89 Loewenstein, M., Jost, H., Grose, J., Eilers, J., Lynch, D., Jensen, S. and Marmie, J. (2002) "Argus: a new instrument for the measurement of the stratospheric dynamical tracers, N₂O and CH₄". *Spectrochimica Acta A*, **58**, 2329–45.
- 90 Fried, A., Crawford, J., Olson, J., Walega, J., Potter, W., Wert, B., Jordan, C., Anderson, B., Shetter, R., Lefer, B., Blake, D., Blake, N., Meinardi, S., Heikes, B., O'Sullivan, D., Snow, J., Fuelberg, H., Kiley, C.M., Sandholm, S., Tan, D., Sachse, G., Singh, H., Faloon, I., Harward, C.N. and Carmichael, G.R. (2003) "Airborne tunable diode laser measurements of formaldehyde during TRACE-P: Distributions and box model comparisons". *Journal of Geophysical Research*, **108**, 8798, 19.1–19.23.
- 91 Webster, C.R., Flesch, G.J., Scott, D.C., Swanson, J.E., May, R.D., Woodward, W. Stephen., Gmachl, C., Capasso, F., Sivco, D.L., Baillargeon, J.N., Hutchinson, A.L. and Cho, A.Y. (2001) "Quantum-cascade laser measurements of stratospheric methane and nitrous oxide". *Applied Optics*, **40**, 321–26.
- 92 Kormann, R., Königstedt, R., Parchatka, U., Lelieveld, J. and Fischer, H. (2005) "QUALITAS: A mid-infrared spectrometer for sensitive trace gas measurements based on quantum cascade lasers in CW operation". *The Review of Scientific Instruments* **76**, 075102.
- 93 Jiménez, R., Herndon, S., Shorter, J.H., Nelson, D.D., McManus, J.B. and Zahniser, M.S. (2005) Atmospheric trace gas measurements using a dual quantum-cascade laser mid-infrared absorption spectrometer, (Novel In-Plane Semiconductor Lasers IV). *Proceedings of SPIE*, Vol. 5738, SPIE, Bellingham, 318–31.
- 94 Richter, D. and Weibring, P. (2006) "Ultra-high precision mid-IR spectrometer I: difference-frequency generation source design". *Applied Physics B*, **82**, 479–86.
- 95 Wert, B.P., Fried, A., Rauenbuehler, S., Walega, J. and Henry, B. (2003) "Design and performance of a tunable diode laser absorption spectrometer for airborne formaldehyde measurements". *Journal of Geophysical Research*, **108** (D12), 4350.
- 96 Roller, C.B., Tittel, F.K., Fried, A., Walega, J., Weibring, P. and Richter, D. (2005) "Advances in the Performance Assessment of a Tunable Diode Laser Absorption Spectrometer for Airborne Measurements of CH₂O", Proceedings of the Conference on Laser and Electro-Optics CLEO 2005, Baltimore, 22-27/05/2005, 1212–14.
- 97 Kormann, R., Fischer, H., Gurk, C., Helleis, F., Klüpfel, Th., Königstedt, R., Parchatka, U. and Wagner, V. (2002) "Application of TRIS-TAR, a three-laser tunable diode laser absorption spectrometer during MINATROC". *Spectrochimica Acta, Part A*, **58**, 2489–98.
- 98 Kerstel, E. (2004) Isotope ratio infrared spectrometry in *Handbook of Stable Isotope Analytical Techniques*, chapter 34, (ed P.A. Groot), Elsevier, Amsterdam, pp. 759–87.
- 99 Werle, P., Dyroff, C., Zahn, A., Mazzinghi, P. and D'Amato, F. (2005) "A new concept for sensitive in-situ stable isotope ratio infrared spectroscopy based on sample modulation". *Isotopes in Environmental and Health Studies*, **41**, 323–33.